

Asperomagnetic order in diluted magnetic semiconductor (Ba,Na)(Zn,Mn)₂As₂

Gangxu Gu, Guoqiang Zhao, Chaojing Lin, Yongqing Li, Changqing Jin, and Gang Xiang

Citation: *Appl. Phys. Lett.* **112**, 032402 (2018); doi: 10.1063/1.5010988

View online: <https://doi.org/10.1063/1.5010988>

View Table of Contents: <http://aip.scitation.org/toc/apl/112/3>

Published by the [American Institute of Physics](#)

Articles you may be interested in

[Tuning the interfacial charge, orbital, and spin polarization properties in La_{0.67}Sr_{0.33}MnO₃/La_{1-x}Sr_xMnO₃ bilayers](#)

Applied Physics Letters **112**, 032401 (2018); 10.1063/1.5011172

[Modulated spin orbit torque in a Pt/Co/Pt/YIG multilayer by nonequilibrium proximity effect](#)

Applied Physics Letters **112**, 022402 (2018); 10.1063/1.5006115

[Influence of MgO barrier quality on spin-transfer torque in magnetic tunnel junctions](#)

Applied Physics Letters **112**, 022406 (2018); 10.1063/1.5005893

[Spin-orbit beams for optical chirality measurement](#)

Applied Physics Letters **112**, 031101 (2018); 10.1063/1.5008732

[High-performance gap-closing vibrational energy harvesting using electret-polarized dielectric oscillators](#)

Applied Physics Letters **112**, 032901 (2018); 10.1063/1.5004254

[Interface-induced perpendicular magnetic anisotropy of Co nanoparticles on single-layer h-BN/Pt\(111\)](#)

Applied Physics Letters **112**, 022407 (2018); 10.1063/1.5010836

High Vacuum Performance

The expanded family of TwisTorr FS
Turbo Pumps

See the
new pumps



Asperomagnetic order in diluted magnetic semiconductor (Ba,Na)(Zn,Mn)₂As₂

Gangxu Gu,^{1,2} Guoqiang Zhao,^{2,3} Chaojing Lin,^{2,3} Yongqing Li,^{2,3,a)} Changqing Jin,^{2,3,b)} and Gang Xiang^{1,c)}

¹College of Physical Science and Technology, Sichuan University, Chengdu 610064, China

²Beijing National Laboratory of Condensed Matter Physics, Institute of Physics, Chinese Academy of Sciences, Beijing 100190, China

³School of Physical Sciences, University of Chinese Academy of Sciences, Beijing 100049, China

(Received 28 October 2017; accepted 29 December 2017; published online 16 January 2018)

We report an investigation of magnetic ordering in (Ba,Na)(Zn,Mn)₂As₂ (BNZMA) single crystals, a type of II-II-V magnetic semiconductor based on BaZn₂As₂, with a combination of magnetic, electron transport, and spin polarization measurements. At temperatures above 90 K, the susceptibility is found to follow the Curie-Weiss law with a Curie-Weiss temperature of 16 K. At low temperatures, both the dc and ac susceptibilities exhibit spin-glass-like features and the electron spin polarization is determined to be $48 \pm 8\%$ using Andreev reflection spectroscopy. Our experimental results suggest that the ground state of BNZMA has an asperomagnetic order, an intermediate regime between a ferromagnet and a canonical spin glass. Such a partially spin polarized glassy phase can be attributed to the competition between the short range antiferromagnetic superexchange interaction and the long range ferromagnetic/antiferromagnetic exchange interactions mediated by high-density holes. *Published by AIP Publishing.*

<https://doi.org/10.1063/1.5010988>

In the past few decades, diluted magnetic semiconductors (DMSs) have received a lot of attention because of their potential in spintronic applications.^{1–4} Much of the work has been focused on whether the ferromagnetic (FM) order can be achieved at room temperature in a DMS. Thanks to enormous experimental efforts worldwide, the FM ordering temperature (T_C) of (Ga,Mn)As, the prototype III-V DMS, has been improved from 60 K (Ref. 1) in 1996 to over 190 K in 2008 by optimizing the thin film growth process⁵ and by introducing post-growth techniques such as low temperature annealing,^{6,7} electron irradiation,⁸ and structural engineering at the nanometer scale.⁹ Further increasing T_C in (Ga,Mn)As, however, seems to be a formidable task due to the low solubility of Mn in GaAs as well as the difficulty in eliminating interstitial Mn ions.⁴ While the efforts on realizing room temperature DMS have been expanded to many other materials,^{10,11} a recently reported II-II-V compound, (Ba_{1-x}K_x)(Zn_{1-y}Mn_y)₂As₂ (BKZMA),¹² offers a promising route toward high T_C magnetic semiconductors. Unlike (Ga,Mn)As, in which the Mn doping simultaneously introduces magnetic moments and mobile carriers into the host material, the charge and spin degrees of freedom in BKZMA can be separately controlled by substitution of both Ba and Zn ions. Curie temperature as high as 230 K has been reported in polycrystalline bulk samples of BKZMA.¹³ BKZMA and the related II-II-V compounds therefore render an appealing model system to gain deep insights into the magnetic interactions and magnetic orderings in DMSs.

Despite the advantages mentioned above, the magnetic properties of BKZMA are still far from perfect. In both

polycrystalline and single-crystalline samples, the zero-field-cooled (ZFC) magnetization was found deviating strongly from the field-cooled (FC) magnetization below a certain temperature.^{12,14} In Ref. 12, such a deviation is attributed to strong magnetic anisotropy in BKZMA (evidenced by coercive fields up to $\mu_0 H_c \sim 1$ T). However, in a subsequent work, Man *et al.* observed a similar bifurcation phenomena in polycrystalline Ba(Zn_{1-2x}Mn_xCu_x)₂As₂ samples.¹⁵ Based on a detailed set of ac susceptibility measurements, they concluded that a transition from the FM phase to a spin glass phase takes place when the temperature drops below 35 K. Since there also exist other similarities in the physical properties of BKZMA and Ba(Zn_{1-2x}Mn_xCu_x)₂As₂, further work is hence necessary to elucidate the nature of magnetic ordering in this family of DMSs.

In this letter, we report a detailed investigation of the magnetic and transport properties of (Ba_{1-x}Na_x)(Zn_{1-y}Mn_y)₂As₂ (BNZMA) single crystals. The spin-glass-like bifurcation behavior is also observed in the ZFC and FC dc susceptibilities (χ_{ZFC} and χ_{FC}) at low temperatures. The magnetic properties in BNZMA are further studied with the measurements of ac susceptibility, electron transport, and Andreev reflection spectroscopy. The experimental results suggest that there is a transition from the paramagnetic to asperomagnetic phase at a temperature close to the bifurcation point.

BNZMA single crystals were synthesized using the flux technique.¹⁴ The real atom ratio, (Ba_{0.907}Na_{0.093})(Zn_{0.819}Mn_{0.181})₂As₂, is determined consistently by inductively coupled plasma mass spectrometry and energy dispersive X-ray analysis. The space group of BNZMA is 14/mmm [Fig. 1(a)], the same as its parent compound BaZn₂As₂. Figure 1(b) shows the X-ray diffraction (XRD) pattern of a typical BNZMA single crystal. Only peaks of (0 0 2n) are

^{a)}Electronic mail: yqli@iphy.ac.cn

^{b)}Electronic mail: jin@iphy.ac.cn

^{c)}Electronic mail: gxiang@scu.edu.cn

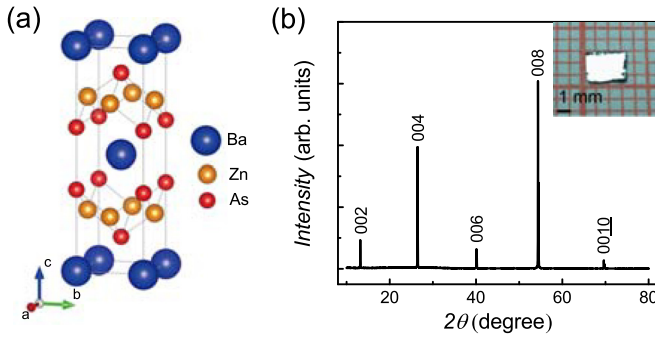


FIG. 1. Crystalline structure of BNZMA. (a) A sketch of the lattice structure of BaZn_2As_2 . In BNZMA, Na and Mn ions presumably substitute Ba and Zn ions, respectively. (b) X-ray diffraction pattern of a BNZMA single crystal collected at room temperature. The inset is an optical image of this sample.

visible, indicating a good crystal quality. The lattice parameters $a = 4.1172(2)$ Å and $c = 13.433(5)$ Å of BNZMA are determined from the refinement of Single Crystal XRD, slightly less than $a = 4.1387(8)$ Å and $c = 13.463(3)$ Å for BKZMA.

Figure 2(a) shows the temperature dependences of χ_{ZFC} and χ_{FC} of a BNZMA single crystal obtained with an external field of $H = 500$ Oe. At high temperatures, χ_{ZFC} and χ_{FC} are identical to each other. As shown in Fig. 2(b), they

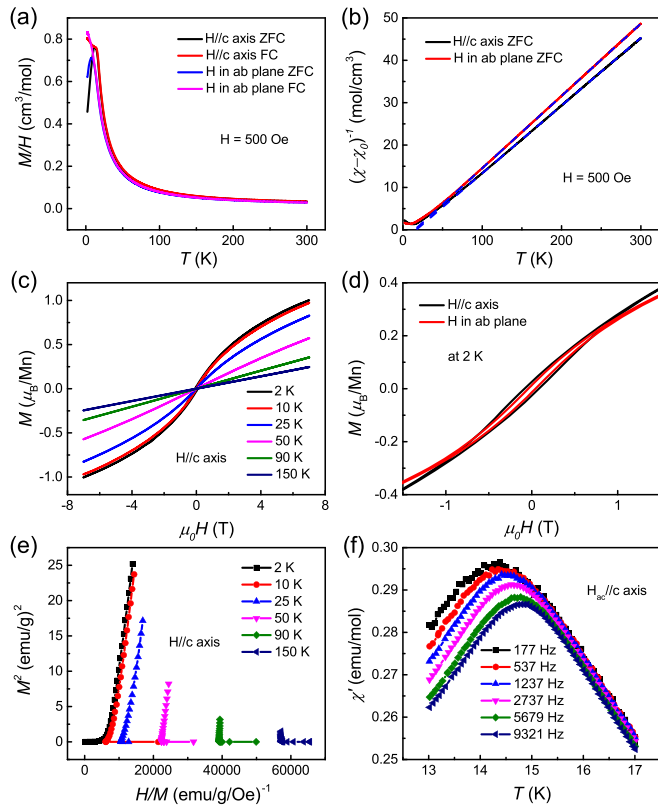


FIG. 2. Magnetic properties of BNZMA. Temperature dependence of (a) the ZFC and FC dc susceptibility ($\chi = M/H$) and (b) the inverse susceptibility. In panels (a) and (b), an external magnetic field of $H = 500$ Oe is applied either parallel or perpendicular to the c -axis. The dashed lines in panel (b) are the fits to the Curie-Weiss law. (c) Magnetization M plotted as a function of H ($M(H)$), which is parallel to the c -axis. (d) $M(H)$ at $T = 2$ K for both parallel and perpendicular field orientations. (e) Arrott plot for $H//c$, which shows no signature for FM ordering. (f) Temperature dependence of the real part of ac susceptibility χ' at different frequencies. The ac field is applied parallel to the c -axis.

follow the Curie-Weiss law $(\chi - \chi_0)^{-1} = (T - \theta)/C$ at $T > 90$ K, where χ_0 is a temperature independent term, C is the Curie constant, and θ is the Curie-Weiss temperature. A linear fit of the ZFC data yields $\theta \sim 16$ K and an effective magnetic moment of about $3.33 \mu_B/\text{Mn}$. At low temperatures, χ_{ZFC} no longer increases with decreasing temperature and a maximum appears at 12 K (8 K) in the fields parallel (perpendicular) to the c axis. In contrast, χ_{FC} continues to increase with decreasing temperature for both field orientations. Similar bifurcation behavior of χ_{ZFC} and χ_{FC} has also been observed in BKZMA single crystals¹⁴ as well as in polycrystalline BKZMA and $\text{Ba}(\text{Zn}_{1-2x}\text{Mn}_x\text{Cu}_x)_2\text{As}_2$ samples.^{12,15}

Figure 2(c) shows that the magnetization M of the BNZMA sample does not saturate in applied fields up to $\mu_0 H = 7$ T and at temperatures as low as 2 K. The linear M - H curves at $T > 90$ K indicate a paramagnetic phase. At low temperatures, the M - H curves become nonlinear and hysteretic. The coercive fields are about 750 Oe and 400 Oe at $T = 2$ K for $H//c$ and $H \perp c$, respectively [Fig. 2(d)]. These values are much smaller than those of the BKZMA single crystals with similar doping concentrations (5.3 kOe for $H//c$),¹⁴ implying a much weaker magnetic anisotropy in BNZMA. The Arrott plots (M^2 vs H/M) with all curves intersecting the horizontal axis at $H/M > 0$ [Fig. 2(e)] further suggest that there is no well-defined long-range FM order in BNZMA down to 2 K.

The ac susceptibility of the BNZMA sample has also been measured at various frequencies to probe the origin of the bifurcation behavior. As shown in Fig. 2(f), the peak position of the real part of ac susceptibility, χ' , shifts to higher temperature with increasing frequency. Similar results have been obtained in $\text{Ba}(\text{Zn}_{1-2x}\text{Mn}_x\text{Cu}_x)_2\text{As}_2$ and many other magnetic materials.^{15–17} This is often ascribed to the formation of spin glass ordering, which originates from spin frustrations due to the competition between FM and antiferromagnetic (AFM) interactions.^{18,19} According to the theory developed by Glasbrenner *et al.*,²⁰ in the II-II-V DMSs, i.e., BNZMA, the nearest neighbor superexchange interactions between Mn ions are AFM, while the carrier mediated interactions are FM. It is hence not surprising to observe the spin-glass-like behavior in this family of DMSs. Nonetheless, it is noteworthy that the FC susceptibility in BNZMA continues to increase as the temperature is dropped below the bifurcation point [Fig. 2(a)]. In contrast, χ_{FC} in a canonical spin glass would remain constant below the freezing temperature T_f (i.e., the bifurcation point).¹⁹

Further insight into the magnetic order in BNZMA can be gained from the magnetotransport measurements [Fig. 3(a)]. Figure 3(b) shows the magnetoresistance (MR) data at temperatures $T = 2$ –150 K. The MR, defined as $\text{MR} = [R_{xx}(B) - R_{xx}(0)]/R_{xx}(0)$, remains negative up to the highest magnetic field (9 T) and exhibits no signature of saturation. The magnitude of MR increases with decreasing temperature and reaches about 26% at $B = 9$ T and $T = 2$ K. Similar negative MRs have been observed in other magnetic semiconductors, such as (Eu,Gd)Se²¹ and BKZMA,¹⁴ can be attributed to reduced spin-dependent scatterings in higher magnetic fields.

As shown in Fig. 3(c), the unsaturated magnetization is also manifested in the Hall effect measurements. At low temperatures, the shape of Hall resistivity curves resembles that

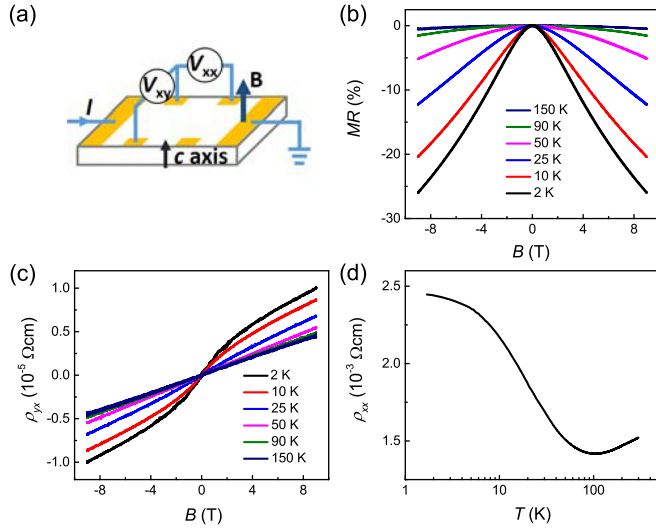


FIG. 3. Transport properties of the BNZMA single crystal. (a) Sketch of the measurement setup. The current flows in the *a*-*b* plane. (b) MRs at temperatures between 2 K and 150 K. (c) Hall resistivity ρ_{yx} for the same set of temperatures. (d) Temperature dependence of longitudinal resistivity ρ_{xx} of BNZMA.

of the $M(H)$ curves [Fig. 2(c)]. This suggests that the Hall resistivity ($\rho_{yx} = R_0B + R_sM$) is dominated by the anomalous Hall effect (AHE). Above 90 K, ρ_{yx} has a linear dependence on the magnetic field. Since M becomes smaller as the temperature is increased, R_sM decreases rapidly with increasing temperature. At $T = 150$ K, AHE is negligible and a hole density of $p = 1.3 \times 10^{21} \text{ cm}^{-3}$ is extracted.

Figure 3(d) depicts the temperature dependence of the longitudinal resistivity ρ_{xx} of the BNZMA sample. At high temperatures, ρ_{xx} becomes smaller with decreasing temperature. Such a metallic behavior is commonly seen in heavily doped degenerate semiconductors. However, ρ_{xx} begins to increase rapidly as the temperature drops below ~ 100 K. The resistivity nearly doubles when temperature drops to ~ 13 K, below which ρ_{xx} increases at a much slower rate. It is noteworthy that this temperature is comparable to $\theta \sim 16$ K and $T_f \sim 12$ K. The large resistivity upturn below 100 K probably originates from spin-related phenomena, since the temperature dependence of dc susceptibility deviates from the Curie-Weiss law roughly in the same temperature range. Other mechanisms such as weak localization can be ruled out since the onset temperature of the ρ_{xx} upturn is too high to be attributed to the phase coherent process. It is notable that similar temperature dependence of ρ_{xx} has been observed in polycrystalline BKZMA samples under high pressure (e.g., 15.8 GPa), where the FM order is suppressed.²² The strong disorder from the large density of randomly located ionized impurities (Na^+ ions) might also play an important role in enhancing the carrier scatterings at low temperatures.

Additional information on the low- T spin structure in BNZMA can be obtained with the Andreev reflection spectroscopy measurements shown in Fig. 4. This technique,²³ which can be performed with either point contact or planar geometry, has been proven very effective in measuring the spin polarizations in a wide range of magnetic materials, including FM metals (e.g., Ni and CrO_2)²³ and magnetic semiconductors, e.g., $(\text{Ga,Mn})\text{As}$,²⁴ EuS ,²⁵ EuO ,²⁶

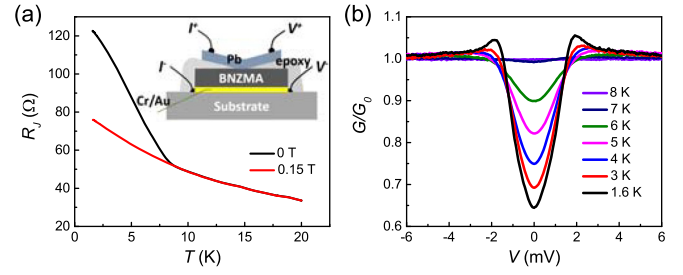


FIG. 4. Andreev reflection spectroscopy measurement. (a) Temperature dependences of the junction resistances of a Pb/BNZMA heterostructure (sample J1) with $B = 0$ and 0.15 T. The inset is a sketch of the Pb/BNZMA planar junction. (b) G/G_0 spectra at $T = 1.6$ –8 K for the sample.

Mn-doped ZnO ,²⁷ and HgCr_2Se_4 .²⁸ It has been shown that the high interface quality (including high transparency and weak inelastic scattering) in superconductor/ferromagnet heterojunctions is important for realizing a reliable determination of spin polarization.^{29–31} Because of the layered structure of BNZMA, high quality Andreev heterojunctions can be readily fabricated by depositing a Pb film on a freshly cleaved surface. In this work, the measurements of the junction resistance (R_J) and differential conductance ($G = dI/dV$) were carried out with the four-point device geometry in which a junction area is about $0.2 \times 0.2 \text{ mm}^2$ [inset of Fig. 4(a)]. The amplitude of the ac current was kept sufficiently small so that the heating and other spurious effects can be excluded. The obtained conductance spectra (i.e., G as a function of the dc bias V across the junction) in the zero magnetic field are normalized with those recorded in a magnetic field of $B = 0.15$ T, which fully suppresses the superconductivity in the device. Figure 4(a) shows the temperature dependences of R_J at $B = 0$ and 0.15 T for sample J1. The two R_J begin to diverge as the temperature drops to the superconducting transition temperature T_C of Pb. Figure 4(b) displays a set of normalized differential conductance (G/G_0) spectra for sample J1, in which the coherence peaks of Pb can be seen clearly. As the temperature increases, the normalized subgap conductance increases gradually and reaches nearly unity for temperatures close to T_C .

Figure 5 shows the G/G_0 spectra for four Pb/BNZMA junctions with the junction resistance $R_J = 75$ –900 Ω at $T < 2$ K and the best fits to the modified Blonder-Tinkham-Klapwijk (BTK) theory.^{32–34} The fits require the use of four parameters: superconducting gap Δ , barrier strength parameter Z , spin polarization P , and inelastic quasiparticle broadening parameter Γ .³⁵ The fitted curves agree very well with the experimental ones, and the extracted P values are in the range of 40% to 57%, with an average value of $P = 48 \pm 8\%$. Other parameters also converge on a narrow range. The obtained Z values (0.28–0.37) are relatively small, implying the good transparency of the interface. The fittings yield $\Delta = 1.2$ –1.43 meV, and the deviations from the BCS gap of Pb (1.4 meV) are possibly due to the interface intermixing.³⁶ The obtained inelastic scattering parameters $\Gamma = 0.6$ –0.75 meV are large but still less than the superconducting gap, supporting the reliability of the extracted P . Interestingly, the average spin polarization is not much lower than $P = 66\%$ obtained for the BKZMA single crystals using the same technique.¹⁴

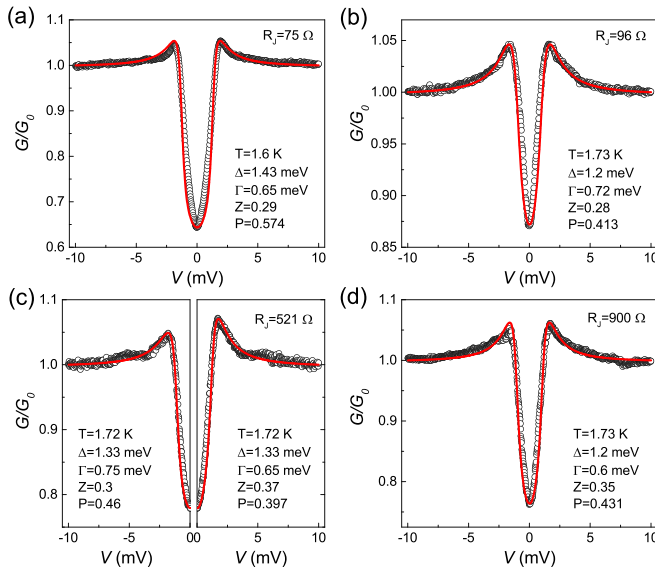


FIG. 5. Spin polarization in BNZMA. Normalized differential conductance spectra of four Pb/BNZMA junctions [samples J1-J4, shown in panels (a)–(d)] at $T < 2$ K. The data (open circles) are fitted to the modified BTK theory (solid lines) with four fitting parameters described in the text.

The coexistence of the partial spin polarization, the positive Curie-Weiss temperature, and the spin-glass-like behavior in susceptibility suggests a complex spin structure in the ground state of BNZMA. The substantial spin polarization and the positive Curie-Weiss temperature (albeit not very large) indicate that the FM interactions are stronger than the AFM counterparts at an overall level. The ground state of BNZMA is thus not a canonical spin glass, which would require equal strengths for the FM and AFM interactions. On the other hand, the FM interactions in BNZMA are not strong enough to establish a long-range FM order, as suggested by the Arrott plot as well as the concave-shaped M - T curve. The low- T magnetic order in BNZMA is therefore in an intermediate regime between the FM phase and the canonical spin glass. This is known as the asperomagnetism,¹⁹ in which some properties resemble those of either a spin glass or a ferromagnet, whereas others exhibit features of the crossover between these two phases. For instance, the low field dependence of magnetization is like a ferromagnet, whereas the high field magnetization does not saturate due to the competition from AFM interactions.¹⁹ This is exactly what happens to BNZMA (Fig. 2).

Finally, it is noted that replacing Na-doping with the same amount of K-doping results in negligible changes in the lattice constants. Therefore, the weaker FM order in BNZMA cannot be attributed to the chemical pressure.^{22,37} It is rather the consequence of the higher density of holes in BNZMA ($1.3 \times 10^{21} \text{ cm}^{-3}$) than that in BKZMA ($5 \times 10^{20} \text{ cm}^{-3}$). According to previous studies, increasing the hole density to a level comparable to the Mn concentration can enhance the AFM portion of the oscillatory Ruderman-Kittel-Kasuya-Yosida (RKKY) interactions.^{38,39}

In summary, by a combination of magnetization, ac susceptibility, electron transport, and Andreev reflection spectroscopy measurements, we have identified an asperomagnetic phase for the ground state of BNZMA. In other words, the sample can be characterized as a partially spin polarized glassy

magnetic semiconductor at low temperatures. The asperomagnetic ordering might also be relevant for other II-II-V magnetic semiconductors such as BKZMA and $\text{Ba}(\text{Zn}_{1-2x}\text{Mn}_x\text{Cu}_x)_2\text{As}_2$. However, it should be noted that the spin-glass-like behavior has been attributed to strong magnetic anisotropy in BKZMA.¹² The results obtained in this work demonstrate that very rich spin-related physics can be accessed by utilizing the versatile tunability in the BaZn_2As_2 -based II-II-V DMSs. It remains interesting to see whether a well-defined FM order can be realized at high temperatures while the ground states are kept free from spin frustrations by carefully engineering the composition and microstructure of this family of compounds.

We thank Shaokui Su, Cong Ren, and Peng Xiong for valuable discussions. This work was supported by the National Science Foundation of China (Project Nos. 11374337 and 61425015), the National Key Research and Development Program (Project No. 2016YFA0300600), the National Basic Research Program of China (Project No. 2015CB921102), and the Strategic Initiative Program of Chinese Academy of Sciences (Project Nos. XDB070200 and XDPB0602).

- ¹H. Ohno, A. Shen, F. Matsukura, A. Oiwa, A. Endo, S. Katsumoto, and Y. Iye, *Appl. Phys. Lett.* **69**, 363 (1996).
- ²T. Dietl, H. Ohno, F. Matsukura, J. Cibert, and D. Ferrand, *Science* **287**, 1019 (2000).
- ³I. Žutić, J. Fabian, and S. Das Sarma, *Rev. Mod. Phys.* **76**, 323 (2004).
- ⁴T. Dietl and H. Ohno, *Rev. Mod. Phys.* **86**, 187 (2014).
- ⁵K. Olejnik, M. H. S. Owen, V. Novák, J. Mašek, A. C. Irvine, J. Wunderlich, and T. Jungwirth, *Phys. Rev. B* **78**, 054403 (2008).
- ⁶T. Hayashi, Y. Hashimoto, S. Katsumoto, and Y. Iye, *Appl. Phys. Lett.* **78**, 1691 (2001).
- ⁷S. J. Potashnik, K. C. Ku, S. H. Chun, J. J. Berry, N. Samarth, and P. Schiffer, *Appl. Phys. Lett.* **79**, 1495 (2001).
- ⁸J. Luo, G. Xiang, G. Gu, X. Zhang, H. Wang, and J. Zhao, *J. Magn. Magn. Mater.* **422**, 124 (2017).
- ⁹L. Chen, X. Yang, F. Yang, J. Zhao, J. Misuraca, P. Xiong, and S. von Molnar, *Nano Lett.* **11**, 2584 (2011).
- ¹⁰T. Dietl, *Nat. Mater.* **9**, 965 (2010).
- ¹¹Z. Deng, C. Q. Jin, Q. Q. Liu, X. C. Wang, J. L. Zhu, S. M. Feng, L. C. Chen, R. C. Yu, C. Arguello, T. Goko *et al.*, *Nat. Commun.* **2**, 422 (2011).
- ¹²K. Zhao, Z. Deng, X. C. Wang, W. Han, J. L. Zhu, X. Li, Q. Q. Liu, R. C. Yu, T. Goko, B. Frandsen *et al.*, *Nat. Commun.* **4**, 1442 (2013).
- ¹³K. Zhao, B. Chen, G. Zhao, Z. Yuan, Q. Liu, Z. Deng, J. Zhu, and C. Jin, *Chin. Sci. Bull.* **59**, 2524 (2014).
- ¹⁴G. Q. Zhao, C. J. Lin, Z. Deng, G. X. Gu, S. Yu, X. C. Wang, Z. Z. Gong, Y. Uemera, Y. Q. Li, and C. Q. Jin, *Sci. Rep.* **7**, 14473 (2017).
- ¹⁵H. Man, S. Guo, Y. Sui, Y. Guo, B. Chen, H. Wang, C. Ding, and F. L. Ning, *Sci. Rep.* **5**, 15507 (2015).
- ¹⁶R. Mathieu, P. Nordblad, D. N. H. Nam, N. X. Phuc, and N. V. Khiem, *Phys. Rev. B* **63**, 174405 (2001).
- ¹⁷J. Dho, W. S. Kim, and N. H. Hur, *Phys. Rev. Lett.* **89**, 027202 (2002).
- ¹⁸K. Binder and A. P. Young, *Rev. Mod. Phys.* **58**, 801 (1986).
- ¹⁹J. M. Coey, *Magnetism and Magnetic Materials* (Cambridge University Press, 2010).
- ²⁰J. K. Glasbrenner, I. Žutić, and I. I. Mazin, *Phys. Rev. B* **90**, 140403 (2014).
- ²¹S. Von Molnar and S. Methfessel, *J. Appl. Phys.* **38**, 959 (1967).
- ²²F. Sun, N. N. Li, B. J. Chen, Y. T. Jia, L. J. Zhang, W. M. Li, G. Q. Zhao, L. Y. Xing, G. Fabbri, Y. G. Wang *et al.*, *Phys. Rev. B* **93**, 224403 (2016).
- ²³R. J. Soulen, J. M. Byers, M. S. Osofsky, B. Nadgorny, T. Ambrose, S. F. Cheng, P. R. Broussard, C. T. Tanaka, J. Nowak, J. S. Moodera *et al.*, *Science* **282**, 85 (1998).
- ²⁴J. G. Braden, J. S. Parker, P. Xiong, S. H. Chun, and N. Samarth, *Phys. Rev. Lett.* **91**, 056602 (2003).

- ²⁵C. Ren, J. Trbovic, R. L. Kallaher, J. G. Braden, J. S. Parker, S. von Molnár, and P. Xiong, *Phys. Rev. B* **75**, 205208 (2007).
- ²⁶A. Schmehl, V. Vaithyanathan, A. Herrnberger, S. Thiel, C. Richter, M. Liberati, T. Heeg, M. Ruckerath, L. F. Kourkoutis, S. Muhlbauer *et al.*, *Nat. Mater.* **6**, 882 (2007).
- ²⁷K. A. Yates, A. J. Behan, J. R. Neal, D. S. Score, H. J. Blythe, G. A. Gehring, S. M. Heald, W. R. Branford, and L. F. Cohen, *Phys. Rev. B* **80**, 245207 (2009).
- ²⁸T. Guan, C. Lin, C. Yang, Y. Shi, C. Ren, Y. Li, H. Weng, X. Dai, Z. Fang, S. Yan *et al.*, *Phys. Rev. Lett.* **115**, 087002 (2015).
- ²⁹I. Žutić and S. Das Sarma, *Phys. Rev. B* **60**, R16322 (1999).
- ³⁰N. Auth, G. Jakob, T. Block, and C. Felser, *Phys. Rev. B* **68**, 024403 (2003).
- ³¹Y. Bugoslavsky, Y. Miyoshi, S. K. Clowes, W. R. Branford, M. Lake, I. Brown, A. D. Caplin, and L. F. Cohen, *Phys. Rev. B* **71**, 104523 (2005).
- ³²G. E. Blonder, M. Tinkham, and T. M. Klapwijk, *Phys. Rev. B* **25**, 4515 (1982).
- ³³I. I. Mazin, A. A. Golubov, and B. Nadgorny, *J. Appl. Phys.* **89**, 7576 (2001).
- ³⁴G. T. Woods, R. J. Soulen, I. Mazin, B. Nadgorny, M. S. Osofsky, J. Sanders, H. Srikanth, W. F. Egelhoff, and R. Datla, *Phys. Rev. B* **70**, 054416 (2004).
- ³⁵R. C. Dynes, V. Narayanamurti, and J. P. Garno, *Phys. Rev. Lett.* **41**, 1509 (1978).
- ³⁶P. Chalsani, S. K. Upadhyay, O. Ozatay, and R. A. Buhrman, *Phys. Rev. B* **75**, 094417 (2007).
- ³⁷F. Sun, G. Q. Zhao, C. A. Escanhoela, B. J. Chen, R. H. Kou, Y. G. Wang, Y. M. Xiao, P. Chow, H. K. Mao, D. Haskel *et al.*, *Phys. Rev. B* **95**, 094412 (2017).
- ³⁸P. J. T. Eggenkamp, H. J. M. Swagten, T. Story, V. I. Litvinov, C. H. W. Swüste, and W. J. M. de Jonge, *Phys. Rev. B* **51**, 15250 (1995).
- ³⁹D. Ferrand, J. Cibert, A. Wasiela, C. Bourgognon, S. Tatarenko, G. Fishman, T. Andrearczyk, J. Jaroszyński, S. Kolesnik, T. Dietl *et al.*, *Phys. Rev. B* **63**, 085201 (2001).